

ORIGINAL ARTICLE

Dynamics of uncrystallized water in partially crystallized poly(ethylene glycol)–water mixtures studied by dielectric spectroscopy

Masahiko Miyara, Ikeru Takashima, Kaito Sasaki, Rio Kita, Naoki Shinyashiki and Shin Yagihara

The dielectric relaxation process of water has been investigated for a partially crystallized poly(ethylene glycol) (PEG)–water mixture with PEG concentrations of up to 50 wt% at temperatures between -60 and 25 °C and over the frequency range of 1 MHz to 50 GHz. At subzero temperatures, most of the water is crystallized, and another portion of the water, uncrystallized water (UCW), remains in a liquid state with the polymer in an uncrystallized phase. The relaxation strength, $\Delta\epsilon$, of UCW for all PEG–water mixtures increased abruptly because of the melting of the eutectic of PEG and water. The $\Delta\epsilon$ of UCW for 10–40 wt% PEG–water mixtures increased again because of the melting of ice, whereas the 50 wt% PEG–water mixture did not show any additional increase in $\Delta\epsilon$ because it did not contain enough water to form ice crystals. The relaxation time of UCW in PEG–water mixtures is smaller than those observed in other polymer–water mixtures. The local fluctuation of the PEG chain, which has a smaller relaxation time than those of other polymers in water mixtures, and the characteristic hydration structure around the PEG chain prevent the formation of ice crystals even for water with a small relaxation time.

Polymer Journal (2017) 49, 511–518; doi:10.1038/pj.2017.15; published online 29 March 2017

INTRODUCTION

Water is indispensable for life. Living things in the polar regions keep uncrystallized water (UCW) in it. UCW is present around guest molecules in aqueous systems even at subzero temperatures. Countless melting and crystallization phenomena in aqueous systems have been investigated mainly by thermal analysis. Although the melting and crystallization phenomena are based on the rearrangement of water and solute molecules, the investigation of the dynamics of these phenomena has been too limited. Understanding the dynamics of water related to its melting and crystallization is important not only in the field of material science but also for the development of medical and engineering applications related to low-temperature preservation and/or sustenance of organs and foods.

Poly(ethylene glycol) (PEG) is a synthetic polymer that has various unique properties, and its interaction with water has been studied extensively. Water-soluble PEG is commonly used for industrial, medical, food product and cosmetic applications.¹ The chemical structure of PEG is $\text{HO}-(\text{CH}_2-\text{CH}_2-\text{O})_n-\text{H}$, a linear chain polymer.^{1,2} Although the chemical structure of PEG is similar to those of poly(methylene glycol) and poly(propylene glycol), PEG is highly soluble in water, whereas poly(methylene glycol) and poly(propylene glycol) are insoluble.^{3,4} The oxygen–oxygen distance between the PEG repeat units (2.88 Å) is close to the oxygen–oxygen distance between two water molecules at 25 °C (2.85 Å).³ On the other hand, those of poly(methylene glycol) and poly(propylene glycol) are not close. The high solubility of PEG is the result of hydrogen bond

formation between the oxygen atoms of PEG and the hydrogen atoms of two water molecules. The minimal water content needed to satisfy the basic hydration of PEG seems to be two water molecules per repeat unit of PEG.³

The hydration structure of PEG–water mixtures has been studied by various techniques, such as Raman spectroscopy,² infrared spectroscopy,^{4,5} light scattering,^{6,7} quasi-elastic neutron scattering,⁸ viscosity measurements,⁸ nuclear magnetic resonance measurements,^{9,10} Brillouin scattering,¹¹ adiabatic calorimetry¹² and differential scanning calorimetry (DSC).^{13–20} The interaction of PEG with water, the structure of hydrated PEG molecules and the hydration number of water molecules per repeat unit of PEG have been discussed. From these studies, the hydration number per repeat unit of PEG has been estimated to be 0.9–3.7.

The DSC thermograms of PEG–water mixtures were classified into three groups, namely, low weight-average molecular weight, M_w PEG (M_w of 200–900); medium M_w PEG (M_w of 1000–2000); and high M_w PEG (M_w of 70 000).^{13–15} One endothermic process was observed for the low M_w PEG–water mixtures. In contrast, two endothermic processes were observed for the 10–40 wt% medium and high M_w PEG–water mixtures, whereas one endothermic process was observed for the 50 wt% medium and high M_w PEG–water mixtures. The endothermic peak at higher temperature is caused by the melting of ice. Moreover, the melting temperature decreases with PEG concentration, whereas the temperature of the peak at lower temperature is almost independent of PEG concentration. The endothermic peak on

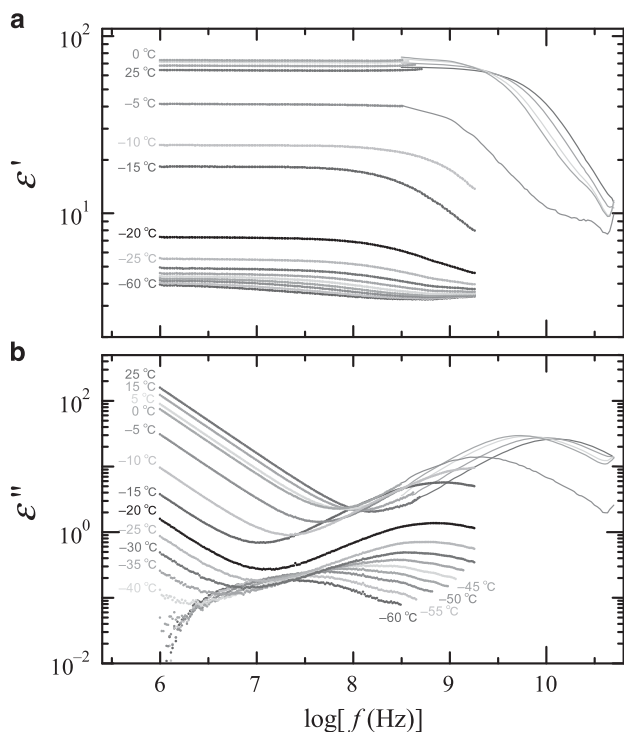


Figure 1 Frequency dependence of the (a) real and (b) imaginary parts of the dielectric function of a 20 wt% poly(ethylene glycol) (PEG)–water mixture at various temperatures from -60 to 0 °C in steps of 5 °C and from 5 to 25 °C in steps of 10 °C. A full colour version of this figure is available at the *Polymer Journal* journal online.

the lower temperature side is characteristic of the melting of a crystalline eutectic of PEG and water at a 0.48 weight fraction of PEG.^{15,17}

In accordance with the DSC results, the melting temperatures were used to draw a phase diagram of the PEG–water mixtures for the various molecular weights of PEG.¹⁴ The hydration numbers of water molecules per repeat unit of PEG estimated from the phase diagram were 1.6, 2.4, 2.7 and 3.3 for PEG–water mixtures with PEG molecular weights of 400, 1540, 4000 and 70 000, respectively. The hydration number increased with increasing PEG molecular weight. There was no eutectic for PEG with a molecular weight of 400. It is impossible for oligomers to reach an ideal crystalline state because of their insufficient chain length to form an ordered helix structure within a crystal. The eutectic cannot be formed for a mixture of PEG with a molecular weight of 400 and 1.6 water molecules per monomer unit because 1.6 is less than the value of 2 needed to satisfy hydration.

The dielectric relaxation process of water was investigated for partially crystallized poly(vinyl pyrrolidone) (PVP)–, poly(ethylene imine) (PEI)–, poly(vinyl methyl ether) (PVME)– and poly(vinyl alcohol) (PVA)–water mixtures at subzero temperatures.²¹ The dielectric relaxation process of UCW was observed at temperatures between -26 and -2 °C. Below the crystallization temperature, T_C , some of the water crystallized, and another portion of the water, UCW, did not crystallize and remained in a liquid state with the polymers in an uncrystallized phase. The relaxation strength, $\Delta\epsilon$, relaxation time, τ , and symmetric broadening shape parameter of the relaxation process, β ($0 < \beta \leq 1$), of UCW changed drastically at T_C . $\Delta\epsilon$ and β decreased with decreasing temperature. τ does not depend on the prepared polymer concentrations and chemical structures of the polymer below T_C . These temperature dependences can be

explained by the crystallization of water and the increase in the polymer concentration in the uncrystallized phase.

In this study, we investigate the dielectric relaxation processes that are mainly caused by the molecular motion of water in the PEG–water mixtures to clarify the dynamics of UCW at subzero temperatures in the presence of two melting events. Thermal analyses were conducted on the melting and crystallization phenomena of the PEG–water mixtures as described above. However, thermal analyses cannot be used to detect UCW. With dielectric measurements, however, we can directly observe the dynamics of UCW via the dielectric relaxation process in the GHz frequency range. Moreover, we can estimate not only the melting temperature and total amount of UCW but also information on the amount of UCW at each temperature and the molecular motions as related to the dielectric relaxation time. Characteristic properties of UCW around PEG are presented.

EXPERIMENTAL PROCEDURES

PEG with a weight-average molecular weight of 8000 was purchased from MP Biomedicals (Santa Ana, CA, USA). Distilled and deionized water with electrical conductivity < 18.2 M Ω cm was obtained from Pure Water Products (Millipore, Darmstadt, Germany, MILL-Q Laboratory). PEG and water mixtures with 10–50 wt% PEG were prepared.

Dielectric measurements of the 10–50 wt% PEG–water mixtures were performed in the frequency range of 1 MHz to 50 GHz at temperatures between -60 and 25 °C on both cooling and heating. We used two instruments to cover the frequency range: an impedance material analyzer (Hewlett Packard, Palo Alto, CA, USA, E4294A, 1 MHz to 1.8 GHz) with a coaxial cylindrical cell having a geometrical capacitance of 0.63 ± 0.03 pF and a network analyzer (Agilent Technologies, Santa Clara, CA, USA, N5230C, 100 MHz to 50 GHz) with a flat-ended coaxial probe (Agilent 85070E). For the measurements with the impedance material analyzer, the temperature was controlled with a digital controller (Shimaden, Tokyo, Japan, SR83) and an immersion cooler (Eyela, Tokyo, Japan, EYELA Cool ECS-80). Dielectric measurements of the cooling process were performed at temperatures from 25 to -60 °C. The sample was cooled by intervals of 5 °C at a cooling rate slower than -0.05 °C min^{-1} . On the other hand, dielectric measurements of the heating process were performed at temperatures from -60 to 25 °C. The sample was heated by intervals of 5 °C at a heating rate slower than 0.2 °C min^{-1} at temperatures from -60 to -30 °C, 1 °C at a heating rate slower than 0.1 °C min^{-1} at temperatures from -30 to 1 °C and 5 °C at a heating rate slower than 0.2 °C min^{-1} at temperatures from 5 to 25 °C. The temperature was maintained for 20 min at an arbitrary temperature. Then, the dielectric measurement was performed for 2 min. For the dielectric measurements with the network analyzer, the temperature was controlled with a thermostat bath (Lauda, Lauda-Königshofen, Germany, PROLINE RP845). Dielectric measurements of the cooling process were performed at temperatures from 25 to -15 °C. The sample was cooled by intervals of 5 °C at a cooling rate slower than -0.3 °C min^{-1} . On the other hand, dielectric measurements of the heating process were performed at temperatures from -15 to 25 °C. The sample was heated by intervals of 1 °C at a heating rate slower than 0.07 °C min^{-1} at temperatures from -15 to 1 and 5 °C at a heating rate slower than 0.3 °C min^{-1} at temperatures from 5 to 25 °C. The temperature was maintained for 20 min at an arbitrary temperature. Then, the dielectric measurement was performed for 10 s.

In the results obtained during the cooling process, the crystallization temperature of the PEG–water mixture was lower than the melting temperature because water is easy to supercool. In addition, the crystallization temperature is more sensitive to the thermal history than the melting temperature. It is difficult to discuss the amount of UCW in the cooling process. In this study, we mainly discuss the results obtained during the heating process.

RESULTS AND DISCUSSION

Dielectric spectra and relaxation processes of UCW

Figure 1 shows the frequency dependences of the real and imaginary parts of the dielectric function for a 20 wt% PEG–water mixture at

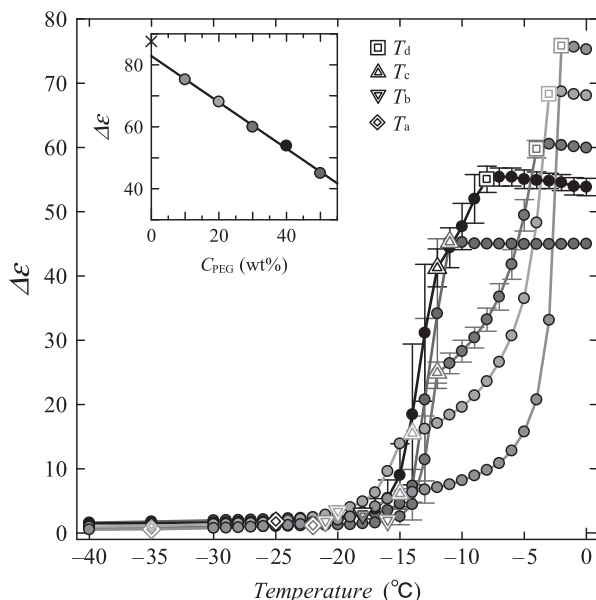


Figure 2 Plots of relaxation strength, $\Delta\epsilon$, against temperature, T , for the poly(ethylene glycol) (PEG)–water mixtures. The symbols indicate the following PEG concentrations: 10 wt% (green solid circles), 20 wt% (yellow solid circles), 30 wt% (red solid circles), 40 wt% (purple solid circles) and 50 wt% (blue solid circles). Double symbols of diamonds, inverted triangles, triangles and squares are the plots at T_a , T_b , T_c and T_d , respectively. The inset shows the plots of $\Delta\epsilon$ against PEG concentration, C_{PEG} (wt %), at 0 °C. The symbol 'x' represents values of $\Delta\epsilon$ for pure water at 0.2 °C taken from Buchner *et al.*²⁴ The solid straight line was plotted using the least-squares method. Error bars denote the minimum and maximum averages calculated for two sets of measurements. No error bars were plotted when the error was smaller than the size of the symbol in the plot. A full colour version of this figure is available at the *Polymer Journal* journal online.

various temperatures. At -60 °C, a dielectric relaxation process with a loss peak at ~ 20 MHz can be observed in Figure 1b. This peak shifts to higher frequencies with increasing temperature. This process is mainly caused by the reorientational motion of water molecules. The local segmental motion of PEG molecules also contributes a small portion of the strength, $<3.0\%$, to this process.²² Two drastic increases in the dielectric constant were observed in the temperature ranges between -20 and -15 °C and between -5 and 0 °C, as shown in Figure 1a. This implies that melting occurs twice.

To characterize the relaxation process, we performed curve fitting on the dielectric spectra. The dielectric spectra of the PEG–water mixtures for all concentrations and temperatures can be reproduced with a simple summation of the Cole–Cole equation²³ and the contribution of dc conductivity as

$$\epsilon(\omega) = \epsilon_{\infty} + \frac{\Delta\epsilon}{1 + (j\omega\tau)^{\beta}} - j \frac{\sigma}{\epsilon_0\omega} \quad (1)$$

Here, ω is the angular frequency, j is the imaginary unit given by $j^2 = -1$, ϵ_0 is the dielectric constant in vacuum, ϵ_{∞} is the high-frequency limit of the dielectric constant and σ is the dc conductivity.

Relaxation time and strength under melting phenomena

The temperature dependences of the relaxation strength and the relaxation time for PEG–water mixtures with various PEG concentrations are shown in Figures 2 and 3, respectively. Figure 3 shows not only the plots of relaxation time for PEG–water mixtures but also those for water mixtures of PVP, PEI, PVME and PVA at various

polymer concentrations quoted from Shinyashiki *et al.*²¹ The plots of the relaxation time of pure water quoted from Buchner *et al.*²⁴ are also plotted. Below 0 °C, the temperature dependences of $\Delta\epsilon$ and τ are complex because melting occurred twice.

To see the details of the complex temperature dependences of $\Delta\epsilon$ and τ , Figure 4 shows (Figure 4a) the temperature dependence of $\Delta\epsilon$, (Figure 4b) relaxation strength differentiated by temperature, $d\Delta\epsilon/dT$, and (Figure 4c) τ of the relaxation process observed for 20 wt% PEG–water mixture as an example. The plot of $d\Delta\epsilon/dT$ shown in Figure 4b is effective in clarifying the change in $\Delta\epsilon$ as it relates to the phase transition during melting, and its temperature dependence mimics the DSC curves. The blue dotted line, i , was drawn from -35 °C, T_a , the temperature at which $d\Delta\epsilon/dT$ deviates from zero, to the high temperature side of -3 °C, T_d , the temperature at which $d\Delta\epsilon/dT$ returns close to zero. This suggests that the ice begins to melt at -35 °C, and this temperature is lower than that at the start of the melting of the eutectic at -22 °C. The red dashed line, e , is the baseline of the melting of the eutectic and is drawn from the start of the steep increase in the melting of the eutectic at -22 °C, T_b , to the end of the peak at -14 °C, T_c . The areas above the baselines ' i ' and ' e ' correspond to the changes in the relaxation strength caused by the melting of ice and the eutectic, respectively. The melting extended the wide temperature range between T_a and T_d . The melting of ice does not occur at a single temperature, and a single melting temperature is not an appropriate way of describing the melting of ice; this is also true for the melting of the eutectic. In this paper, the melting temperature of ice, T_{mi} , is defined as the temperature range between T_a and T_b , and the melting temperature of the eutectic, T_{me} , indicates the temperature range between T_b and T_c . T_{mi} and T_{me} are given by the ranges between the blue dot-dashed lines and red double-dot-dashed lines, respectively, as shown in Figure 4. T_{mi} and T_{me} are listed in Table 1 together with T_a , T_b , T_c and T_d . T_a and T_d are not determined for the 50 wt% PEG–water mixture as no ice crystals were formed in it.

The $\Delta\epsilon$ for a PEG–water mixture comprises the relaxation strength of water, $\Delta\epsilon_w$, and that of PEG, $\Delta\epsilon_p$. The relative contributions of water and PEG to the relaxation strength were estimated as follows. According to the water content (C_{water} (g cm⁻³)) dependence of the relaxation strength of the PEG600–water mixtures at 25 °C, the relaxation strength increases linearly with increasing C_{water} from 9.0 for pure PEG to 73.2 for pure water.²² The C_{water} dependence of the relaxation strength of pure PEG8000 has not been reported yet. At 25 °C, pure PEG600 is liquid, whereas pure PEG8000 is a solid composed of amorphous and crystalline parts. Therefore, it is impossible to obtain the dielectric constants of pure liquid PEG8000 below its melting temperature including room temperature. From the molecular weight dependence of the relaxation strength of pure ethylene glycol oligomers and PEG at 25 °C with the number of repeat units of ethylene glycol oligomers and PEG ranging from 1 to 13, the relaxation strength seems to be constant when the number is above 8. Then, we assume that the relaxation strength of PEG8000 is almost equal to that of PEG600. The estimated contributions of the fractions of the relaxation strength of PEG in the liquid state at temperatures above T_d are 1.3%, 3.0%, 5.0%, 7.6% and 11% for the 10, 20, 30, 40 and 50 wt% PEG–water mixtures, respectively. As shown in Figure 4, above T_d , the 20 wt% PEG–water mixture is liquid. $\Delta\epsilon_w$ is calculated by subtracting $\Delta\epsilon_p$ from $\Delta\epsilon$ for each temperature value ($\Delta\epsilon_w = \Delta\epsilon - \Delta\epsilon_p$). At temperatures between 25 °C and T_b , we assume that the ratio of $\Delta\epsilon_w$ to $\Delta\epsilon_p$ is the same as that at 25 °C. At temperatures between T_d and T_c , microscopic phase separation to ice and noncrystalline phases occurs.^{25,26} The water included in the ice phase cannot contribute to the relaxation process of water, and water

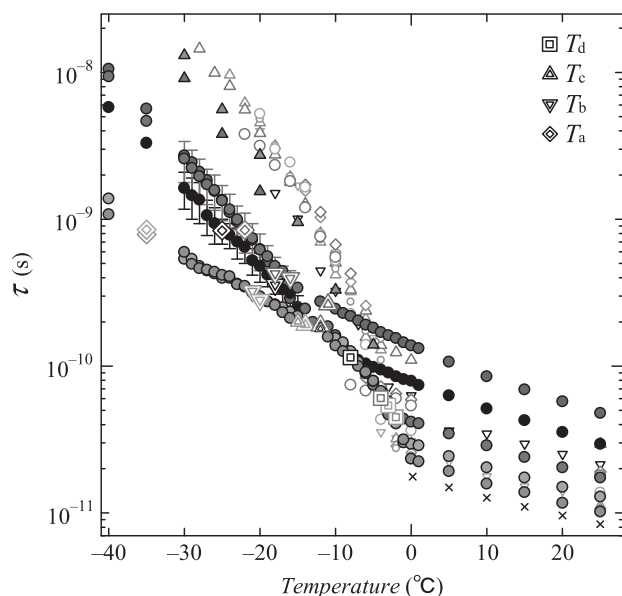


Figure 3 Plots of relaxation time against temperature for poly(ethylene glycol) (PEG)–water mixtures with various PEG concentrations. The symbols indicate the following PEG concentrations: 10 wt% PEG (green solid circles), 20 wt% PEG (yellow solid circles), 30 wt% PEG (red solid circles), 40 wt% PEG (purple solid circles) and 50 wt% PEG (blue solid circles). Double symbols of diamonds, inverted triangles, triangles and squares are the plots at T_a , T_b , T_c and T_d , respectively. The given error bars indicate the minimum and maximum averages derived from the two measurement sets. No error bar was plotted when the error was smaller than the size of the plotted symbol. The relaxation times observed for water and for four polymer–water mixtures with various polymer concentrations measured by time domain reflectometry from Shinyashiki *et al.*²¹ and Buchner *et al.*²⁴ are also plotted. The symbols indicate the following polymers and their concentrations: 20 wt% poly(vinyl pyrrolidone) (PVP; yellow open inverted triangles), 40 wt% PVP (purple open inverted triangles), 10 wt% poly(ethylene imine) (PEI; green open triangles), 30 wt% PEI (red open triangles), 10 wt% poly(vinyl methyl ether) (PVME; green open diamonds), 30 wt% PVME (red open diamonds), 10 wt% poly(vinyl alcohol) (PVA; green open circles), 20 wt% PVA (yellow open circles), 30 wt% PVA (red open circles) and pure water (black crosses). The relaxation times of uncrystallized water (UCW) in PEI–water mixtures measured by impedance material analyzer (IMA) of unpublished results are also plotted. The symbols indicate the PEI concentrations of 10 wt% PEI (green triangles) and 30 wt% PEI (red triangles). A full colour version of this figure is available at the *Polymer Journal* journal online.

and PEG included in the noncrystalline phase contribute to the relaxation strength. Therefore, $\Delta\epsilon$ and $\Delta\epsilon_w$ decrease with decreasing temperature. On the other hand, we assume that $\Delta\epsilon_p$ remains almost constant down to T_c because PEG does not crystallize in this temperature range. Water and PEG form a eutectic at temperatures between T_c and T_b . PEG and water included in the eutectic cannot contribute to the relaxation process. It is impossible to estimate the actual values of $\Delta\epsilon_w$ and $\Delta\epsilon_p$. Below T_c , $\Delta\epsilon$ is contributed by both PEG, $\Delta\epsilon_p$, and water, $\Delta\epsilon_w$, in the noncrystalline phase. Then, we assume that the ratio of $\Delta\epsilon_w$ to $\Delta\epsilon_p$ at temperatures lower than T_c remains the same as that at T_c . The temperature dependences of both $\Delta\epsilon$ and $\Delta\epsilon_w$ for the 20 wt% PEG–water mixture are shown in Figure 4a.

$\Delta\epsilon_w$ in Figure 4a is 0.97 at T_a . $\Delta\epsilon_w$ increases drastically with increasing temperature at ~ -16 °C that corresponds to the peak of $d\Delta\epsilon_w/dT$ at approximately the same temperature shown in Figure 4b. These are caused because of the melting of the eutectic.

According to the DSC results, the endothermic peak caused by the melting of the eutectic is observed for the 20 wt% PEG–water mixture at -16 °C.^{14,15} Above -15 °C, once $d\Delta\epsilon_w/dT$ has dropped off again, $d\Delta\epsilon_w/dT$ gradually increases once more, and this increase becomes steeper up to -3 °C. The peak of $d\Delta\epsilon_w/dT$ at -3 °C caused by melting is also observed. For the 20 wt% PEG–water mixture, the endothermic peak is observed at -2 °C by DSC.^{14,15} This corresponds to the peak of $d\Delta\epsilon_w/dT$ at -3 °C. Above -2 °C, all ice in the system has melted and $\Delta\epsilon$ decreases with increasing temperature. Then, the melting of the ice and eutectic can be distinguished clearly by $d\Delta\epsilon_w/dT$.

As shown in Figure 4c, τ decreases with increasing temperature between -60 and -15 °C. The temperature dependence of τ changes at -15 °C. τ decreases steeply with increasing temperature at temperatures between -15 and -2 °C. The temperature dependence of τ during the melting of ice is stronger than that during the melting of the eutectic.

As shown in Figure 2, $\Delta\epsilon$ increases twice for the 10–40 wt% PEG–water mixtures. On the other hand, $\Delta\epsilon$ increases only once for the 50 wt% PEG–water mixture. The melting of the eutectic is observed at ~ -15 °C for all PEG–water mixtures. Furthermore, the melting of ice is only observed for the 10–40 wt% PEG–water mixtures. This indicates that the 10–40 wt% PEG–water mixtures are composed of three phases: the eutectic, ice crystals and an uncrystallized (liquid) phase. The uncrystallized phases in partially crystallized materials have been called the freeze-concentrated phase. On the other hand, the 50 wt% PEG–water mixture therefore does not contain enough water to form ice crystals. It has been determined that a eutectic is composed of two water molecules per repeat unit of PEG.¹⁶

Above 0 °C, the point at which all PEG–water mixtures are liquid, τ depends on PEG concentration; furthermore, τ is larger in the PEG–water mixtures with higher PEG concentrations, as shown in Figure 3. Below T_d , the temperature dependences of τ are larger than those above T_d because of the melting of the ice and the eutectic. The values of τ are independent of the initial concentrations at ~ -15 °C, just below the point at which all the eutectic is melted and most of the ice does not melt. It means that the structure of water melted from the eutectic does not depend on the initial PEG concentration at temperatures just above T_{me} . For the 10–40 wt% PEG–water mixtures, the values of τ at temperatures between -15 °C and each mixture's T_d lie on a single trace. The narrow range of T_{me} implies that water included in the eutectic has a homogeneous structure. On the other hand, the temperature range of the melting of ice between T_a and T_d is wide, and the change in τ in T_{mi} is larger than that in T_{me} . The water molecules with high mobility are expected to be located far from the PEG chains, and their dynamic and thermal properties as well as their structure are similar to those of pure water. The water molecules with high mobility are expected to crystallize and melt at temperatures close to T_d . In contrast, the water molecules with low mobility are adjacent to the PEG chains and their dynamic and thermal properties and structure are different from those of bulk water. Therefore, the water included in ice in PEG–water mixtures is heterogeneous.

Contributions to $\Delta\epsilon$ of three types of water and PEG concentration in the uncrystallized phase

The water in PEG–water mixtures is classified into three types: 'water included in ice', 'water included in the eutectic' and 'water remaining in the liquid state below T_a ' according to the analysis of Figures 4a and b that follows. The value of $\Delta\epsilon_w$ at T_a is caused by the water that is included in neither the ice nor the eutectic, even at T_a . We define $\Delta\epsilon_l$ as the relaxation strength of the water that remains in the liquid

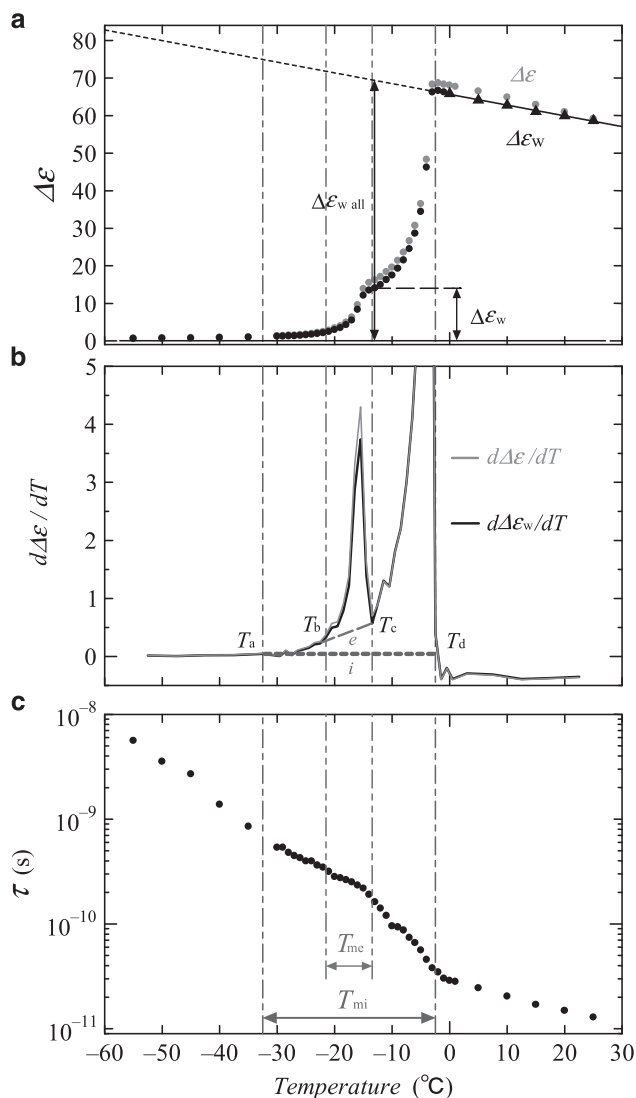


Figure 4 Temperature dependence of (a) relaxation strength, (b) relaxation strength differentiated by temperature and (c) relaxation time for the 20 wt % poly(ethylene glycol) (PEG)–water mixtures during the heating process. The straight solid and dotted lines in (a) are plotted using the least-squares method assuming a linear dependence of $\Delta\epsilon$ on T above 0 °C. (a) The observed relaxation strength, which includes contributions from both water and PEG ($\Delta\epsilon$, green solid circles), the relaxation strength of water ($\Delta\epsilon_w$, black solid circles) and the effect of $\Delta\epsilon_w$ on the cooling process (black solid triangles) are shown. A full colour version of this figure is available at the *Polymer Journal* journal online.

state at T_a . By integrating the value of $d\Delta\epsilon_w/dT$ above the baseline ‘e’ at temperatures between T_b and T_c , the integral value corresponds to the relaxation strength of the water included in the eutectic at T_b and lower, $\Delta\epsilon_e$. Moreover, by integrating the value of $d\Delta\epsilon_w/dT$ above the baseline ‘i’ at temperatures between T_a and T_d and subtracting $\Delta\epsilon_e$, the integral value corresponds to the relaxation strength of the water included in the ice, $\Delta\epsilon_i$.

Figure 5 shows plots of $\Delta\epsilon_i$, $\Delta\epsilon_e$ and $\Delta\epsilon_l$ as functions of C_{water} (g cm^{-3}) for the various PEG–water mixtures. This figure shows the amounts of ice, eutectic and UCW. The black solid circles are the sum of $\Delta\epsilon_i$, $\Delta\epsilon_e$ and $\Delta\epsilon_l$, whereas the green solid circles are the sum of the relaxation strength of water and PEG. The black solid and green dashed straight lines were obtained using the least-squares

method. The black solid line extrapolated to $C_{\text{water}}=0$ is close to 0. The relaxation strength of pure PEG600 at 25 °C²² is indicated by a green double circle, and water at 25 °C²² is indicated by a blue cross. The green dashed line is close to the plotted data point of pure PEG600. The value of $\Delta\epsilon_i$ is 0 when C_{water} is $<0.56 \text{ g cm}^{-3}$. This indicates that there is not enough water to form any ice crystals because most of the water is included in the eutectic. At the more water-rich concentrations, $\Delta\epsilon_i$ increases with increasing C_{water} . On the other hand, $\Delta\epsilon_e$ decreases with increasing C_{water} . For all PEG–water mixtures, $\Delta\epsilon_l$ is markedly smaller than both $\Delta\epsilon_i$ and $\Delta\epsilon_e$.

According to the Kirkwood equation,²⁷ $\Delta\epsilon$ is determined by the magnitude of the dipole moment, the number of molecules in a unit volume that contribute to the relaxation process, the temperature, the Kirkwood structural factor g and the internal electric field. As shown in the inset of Figure 2, $\Delta\epsilon$ at 0 °C is almost proportional to the water content. The structure of water below T_d is expected to be somewhat different from that of water above T_d because water molecules exist at neighboring PEG chains in the uncrystallized phase. However, the $\Delta\epsilon$ of water is almost proportional to the water content of the PEG–water mixture, as shown in Figure 5. Therefore, it is possible to assume that $\Delta\epsilon_w$ below 0 °C is proportional to the density of UCW. The relaxation strength of all the water in the mixture, $\Delta\epsilon_{w \text{ all}}$, below 0 °C can be estimated by extrapolating the plots by assuming a linear dependence of $\Delta\epsilon$ on the temperature above 0 °C, as shown by the dotted lines in Figure 4a. Based on these assumptions, we estimated the PEG concentration in the uncrystallized phase in partially crystallized mixtures, $C_{p,UCP}$, below T_d using Equation (2) that is given as follows:

$$C_{p,UCP} = \frac{100C_p}{C_p + (100 - C_p) \frac{\Delta\epsilon_w}{\Delta\epsilon_{w \text{ all}}}} \quad (2)$$

where C_p is the PEG concentration of the prepared mixture. Below T_c , the value of $C_{p,UCP}$ cannot be obtained because the actual ratio of the contributions of water and PEG to the relaxation strength are unknown. Thus, Equation (2) is valid at temperatures above T_c . In the partially crystallized mixture, the density of the mixture is expected to decrease with the crystal growth. If all the water in the mixture is crystallized, the density decrease will be greatest at 9% for the 10 wt% PEG–water mixture. The densities of the PEG–water mixtures are between 1.00 and 1.09 g cm^{-3} at 25 °C, with higher densities for higher PEG concentrations. The density reduction caused by ice crystallization is partly compensated by the higher density of the higher PEG concentration mixture.²¹ Thus, we treat the densities of mixtures below 0 °C as 1 g cm^{-3} , with an error of $<9\%$. The values of $C_{p,UCP}$ obtained from the dielectric relaxation strengths at T_c just above T_{me} are listed in Table 1.

Figure 6 shows the solid–liquid state diagram of PEG–water mixtures in the temperature range above T_c . At T_c , $C_{p,UCP}$ values are $\sim 55 \text{ wt}\%$, at which all the eutectic is just melted, whereas almost all the ice in the 10–40 wt% PEG–water mixtures remain solid. At temperatures between T_c and T_d , ice gradually melts with increasing temperature, that is, UCW increases with increasing temperature. The data points of the partially crystallized mixtures lie almost on a single trace, that is, the concentration of PEG is the same at the same temperature. When all ice in the 10–40 wt% PEG–water mixtures has melted, $C_{p,UCP}$ returns to the same concentrations of the prepared mixtures, C_p , causing the plots to be vertical lines.

Table 1 The temperature range of the melting of the eutectic, T_{me} , and that of ice, T_{mi} , for PEG–water mixtures and PEG concentration in the uncrystallized phase, $C_{p,UCP}$, as well as the number of water molecules per repeat unit of PEG in the eutectic, n_{we}

C_p (wt%)	Melting temperature ranges				$C_{p,UCP}$ (wt%) at T_c	n_{we}
	Eutectic; T_{me} (°C)		Ice; T_{mi} (°C)			
	T_b	T_c	T_a	T_d		
10	-21	-15	-35 ± 5	-2	63	0.7
20	-22	-14	-35 ± 5	-3	56	1.2
30	-16	-12	-22 ± 2	-4	54	1.6
40	-18	-12	-25 ± 2	-8	49	2.0
50	-18	-11	—	—	51	2.4
Average					55 ± 8	

Abbreviation: PEG, poly(ethylene glycol).

Though not displayed, the error in the temperature is plus or minus 1 °C.

Number of water molecules in the eutectic

The number of water molecules per repeat unit of PEG in the eutectic, n_{we} , can be estimated using Equation (3):

$$n_{we} = \frac{100 - C_{p,UCP,e}}{M_w} \cdot \frac{M_p}{C_{p,UCP,e}} \quad (3)$$

where

$$C_{p,UCP,e} = \frac{100C_p}{C_p + (100 - C_p) \frac{\Delta\epsilon_e}{\Delta\epsilon_{w,all}}}$$

M_w is the molecular weight of a water molecule and M_p is the molecular weight of a repeat unit of PEG. $\Delta\epsilon_e$ in Equation (3) does not include the contribution from the PEG. The values of n_{we} are listed in Table 1. n_{we} increases with increasing PEG concentration. For mixtures with 10, 20 and 30 wt% PEG, the value of n_{we} is <2. When the temperatures of these mixtures fall to approximately T_c and the water is crystallized at that very moment, the majority volume of the mixture is occupied by ice. In this case, fewer water molecules should remain around the PEG chain at a temperature just above T_c ; thus, it is difficult to form the eutectic for all repeat units of PEG below T_c . For mixtures with 40 wt% PEG, just two water molecules per repeat unit of PEG are included in the eutectic. de Vringer *et al.*¹⁶ proposed the idea that the low-temperature hydrate structure of PEG–water mixtures has two hydrogen bonded water molecules between oxygens on neighboring PEG units. The value of n_{we} for 50 wt% PEG–mixtures is 2.4, as listed in Table 1; this n_{we} value agrees with the hydration number of water molecules per repeat unit of PEG obtained from the phase diagram determined by DSC.¹⁴ Huang and Nishinari¹⁴ proposed the idea that when the hydration numbers of the repeat unit of PEG is above two, an intermolecular structure must exist that accommodates more water molecules between the PEG chains. The hydration number of the water molecules per repeat unit of PEG is obtained by thermal analysis from the eutectic point (concentration) in the phase diagrams. Therefore, the concentration dependence of the hydration number was not obtained from the DSC results. Instead, we estimated the value of n_{we} for each PEG concentration using dielectric spectroscopy.

Relaxation time of UCW on the melting phenomenon

Figure 7 shows the relationships among the relaxation time, PEG concentration, C_{PEG} and temperatures of the PEG–water mixtures.

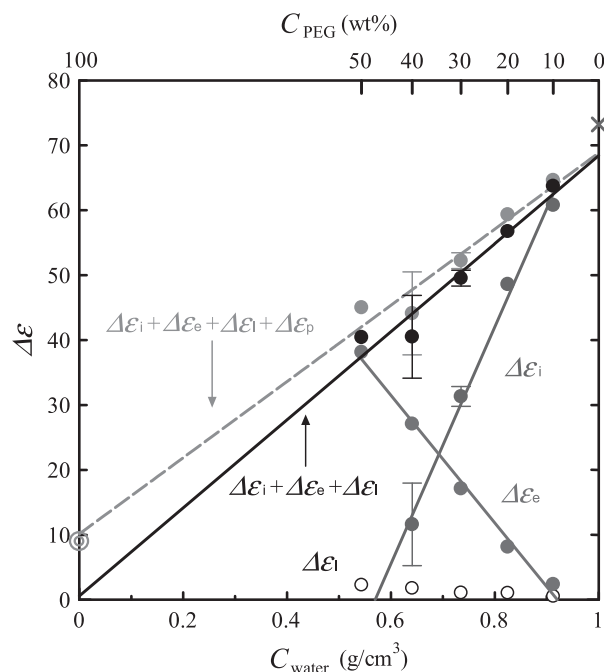


Figure 5 Plots of relaxation strength, $\Delta\epsilon$, against the water content, C_{water} , for the poly(ethylene glycol) (PEG)–water mixtures. The symbols indicate the strength of the water that is included in ice ($\Delta\epsilon_i$, blue solid circles), the eutectic ($\Delta\epsilon_e$, red solid circles), water at T_a ($\Delta\epsilon_i$, open circles), the sum of $\Delta\epsilon_i$, $\Delta\epsilon_e$ and $\Delta\epsilon_i$ (black solid circles), the sum of all relaxation strengths including the relaxation strength of PEG (green solid circles), pure water at 25 °C (black crosses) and pure PEG600 at 25 °C (green double circles). The straight lines are plotted using the least-squares method. The error bars indicate the minimum and maximum averages determined with two measurement sets. No error bars are shown if the error is smaller than the size of the symbol. A full colour version of this figure is available at the *Polymer Journal* journal online.

The colors in the plot represent temperature. The colorless area indicates the temperature range below T_a . The values of τ vary with the PEG concentration. We deduce that a very small amount of water remains in the liquid state below T_a , and this water is included in neither ice nor the eutectic. The environment of this type of water seems to be unpredictably determined, resulting in the variation in τ . The plots with red crosses indicate the relaxation time at T_c , the point at which all the eutectic has melted. The red line is obtained using the least-squares method. At T_c , τ for all concentrations agree within the error. In the red area, there is no eutectic and ice melts gradually with increasing temperature. The plots with blue crosses show the relaxation time at T_b , the temperature at which all ice has melted. The blue curve is drawn as a guide to the eyes. The 10–30 wt% PEG–water mixtures are partially crystallized at -5 °C in the red area and τ is almost constant, whereas the 40 and 50 wt% PEG–water mixtures are liquid in the green area and τ increases with increasing C_{PEG} . The yellow dot-dashed line shows the average value of τ for the 10–30 wt% PEG–water mixtures, and the line crosses the blue solid curve at 35 wt% of PEG. This suggests that the C_{PEG} values of these mixtures at -5 °C are the same at ~35 wt% PEG. This C_{PEG} at -5 °C agrees well with that obtained from the relaxation strength, as shown in Figure 6. On the other hand, the 40 and 50 wt% PEG–water mixtures at -5 °C and all the concentrations above 0 °C are in the liquid state in the green area, and τ increases with increasing C_{PEG} in Figure 7.

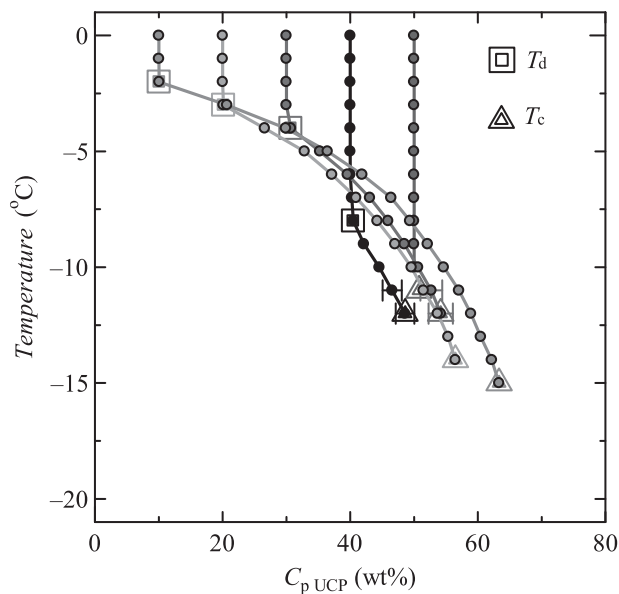


Figure 6 The solid–liquid state diagram plots of the poly(ethylene glycol) (PEG) concentration in the uncrystallized phase and solution $C_{p,UCP}$ against temperature T ($^{\circ}\text{C}$) for PEG–water mixtures. Different symbols indicate different PEG concentrations: 10 wt% (green solid circle), 20 wt% (yellow solid circles), 30 wt% (red solid circles), 40 wt% (purple solid circles) and 50 wt% (purple solid circles). Double symbols of triangles and squares are the plots at T_c and T_d , respectively. Error bars indicate the minimum and maximum averages calculated with two measurement sets. No error bars are shown if the error is smaller than the size of a symbol. A full colour version of this figure is available at the *Polymer Journal* journal online.

The τ of UCW in water mixtures of PEG and other

Figure 3 also includes the relaxation time of water observed in four polymer (PVP, PEI, PVME and PVA)–water mixtures quoted from Shinyashiki *et al.*²¹ The temperature dependence of τ for PEG–water mixtures above 0°C is almost the same as those of four polymer–water mixtures. For the four polymer–water mixtures, the relaxation time of UCW does not depend on the prepared polymer concentrations and chemical structures of the polymer; thus, the plots of τ against temperature lie on a single trace below the melting temperature of water. The independence of τ on the polymer structure was interpreted as whether the water molecules form ice crystals or stay in the liquid phase in a partially crystallized polymer water mixture is determined by the relaxation time (mobility) of water.²¹ The values of τ for the PEG–water mixtures are smaller than those for the four polymer–water mixtures at temperatures below T_d . This implies that the water with a small relaxation time cannot crystallize around the PEG chain. The interaction between PEG and water seems special because of the distance between hydrogen-bonding sites on the PEG chain. It is expected that this special structure of water, even the molecules with a small relaxation time around PEG, prevent its crystallization. For the mixtures with PVP and PVME, the relaxation processes caused by the local segmental motion of the polymer and reorientational motion of water are observed individually in the liquid state.^{28–30} Table 2 shows the frequency ranges in which the relaxation processes can be observed at 25°C . For the mixtures with PVP and PVME, the relaxation process of the polymer can be observed in the MHz range, whereas the relaxation process of water can be observed in the GHz range. The frequency ranges of the molecular motion of a polymer and water differ by three orders of magnitude. The relaxation process originating from the local chain motion of PEI and PVA in the water mixtures has

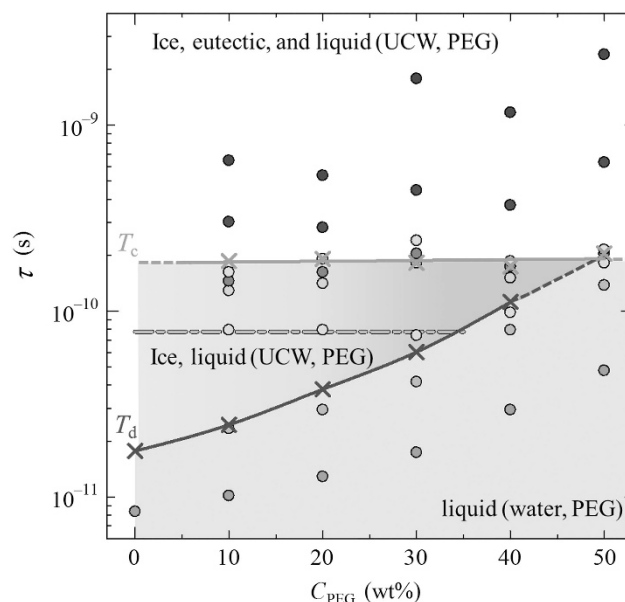


Figure 7 Plot of relaxation time, τ , against poly(ethylene glycol) (PEG) concentration, C_{PEG} , for the various PEG–water mixtures. The symbols indicate various temperatures: -30°C (purple solid circles), -20°C (blue solid circles), -14°C (aqua solid circles), -13°C (green solid circles), -12°C (yellow-green solid circles), -5°C (yellow solid circles), 0°C (orange solid circles), 25°C (red solid circles), T_c (red crosses) and T_d (blue crosses). The red line indicating T_c is obtained using the least-squares method and the blue line indicating T_d is drawn as a guide to the eyes. The yellow dot-dashed line shows the average value of τ at -5°C for 10–30 wt% PEG–water mixtures. A full colour version of this figure is available at the *Polymer Journal* journal online.

Table 2 Frequency ranges of the loss peaks of the relaxation processes caused by PVP, PVME and water for polymer–water mixtures at 25°C

	10–50 wt%		30–50 wt%		10–50 wt%
	PVP–water		PVME–water		PEG–water
	mixtures ²⁸		mixtures ²⁹		mixtures
Relaxation	PVP	Water	PVME	Water	PEG and water
Frequency ranges	2–12 MHz	7–12 GHz	60–100 MHz	4–8 GHz	3–16 GHz

Abbreviations: PEG, poly(ethylene glycol); PVME, poly(vinyl methyl ether); PVP, poly(vinyl pyrrolidone).

not yet been reported. For PEI–water mixtures, the relaxation process of PEI is observed in the low-frequency side of that of water, according to our unpublished results. We consider that the relaxation process of PVA is expected to be present on the low-frequency side of relaxation process of water (the same as other polymer–water mixtures). For PEG–water mixtures, a single relaxation process is observed in the GHz range. This process originates not only from the reorientational motion of water molecules but also from the local segmental motion of PEG molecules. This means that the relaxation times of PEG and water are similar. The fluctuation of the PEG chain with smaller τ does not provide enough time for water to form ice crystals around the PEG chain. Then, the PEG chain makes it possible to keep water with rather small τ as UCW. The unique relationships between PEG and water because of (1) the characteristic length, which fits two water molecules,

of neighboring hydrogen-bonding sites on PEG chain, and (2) the small relaxation time of the local segmental motion of PEG chain can be considered as the cause of the small relaxation time of UCW in PEG-water mixtures. To date, only four polymer-water mixtures can be used for comparison of the τ of UCW. To judge the genuine mechanism of the small relaxation time of UCW in PEG-water mixtures, experimental results of various types of water mixtures of polymers and biopolymers are needed.

CONCLUSION

The dielectric relaxation of UCW in 10–50 wt% PEG-water mixtures in the frequency range of 1 MHz to 50 GHz and in the temperature range of -60 to 25 °C were reported. UCW can be classified into three types of water: ‘water included in ice’, ‘water included in the eutectic’ and ‘water remaining in the liquid state’. The dynamic properties of these types of water were clarified. Based on our results, we concluded the following.

1. A dielectric relaxation process that originates mainly from the reorientational motion of water was observed in all PEG-water mixtures at temperatures between -60 and 25 °C. The local chain motion of PEG contributes a small amount to this process.
2. The increase in $\Delta\epsilon$ caused by the melting of the eutectic composed of water and PEG is observed for all PEG-water mixtures at ~ -15 °C. Melting of ice is observed for the 10 to 40 wt% PEG-water mixtures at -35 to -2 °C. The 50 wt% PEG-water mixture does not show any melting of ice. Even below the melting temperature of the eutectic, a small amount of UCW and PEG is not included in ice and the eutectic. Importantly, the two melts of ice and the eutectic can be distinguished clearly by the two peaks of $d\Delta\epsilon/dT$.
3. At T_c , the values of τ of UCW in the PEG-water mixtures with various concentrations are the same. This means that the structure of UCW, which is included in the eutectic below T_c , does not depend on the initial PEG concentration.
4. The number of water molecules per repeat unit of PEG in the eutectic, n_{we} , are 0.7–2.4 in 10–50 wt% PEG-water mixtures that increases with PEG concentration. The range of n_{we} includes two; thus, two water molecules can directly bind to each repeat unit of PEG. The value of n_{we} for the 50 wt% PEG-water mixture is 2.4, and this is in agreement with the hydration number determined by DSC.
5. The values of τ of UCW in the PEG-water mixtures are smaller than those in the four polymer-water mixtures at temperatures below T_d . The unique relationships between PEG and water, the characteristic length, which fits two water molecules, of the neighboring hydrogen-bonding sites on PEG chain and a small relaxation time of the local segment motion of PEG chain are expected to be the origin.

CONFLICT OF INTEREST

The authors declare no conflict of interest.

ACKNOWLEDGEMENTS

This work was partly supported by JSPS KAKENHI Grant Numbers 16K05522 and 15K13554, and MEXT-Supported Program for the Strategic Research Foundation at Private Universities, 2014–2018.

- 1 Powell, G. M. in *Handbook of Water-Soluble Gums and Resins* (ed. Davidson R. L.) Ch. 18, 1–31 (McGrawHill, New York, 1980).
- 2 Maxfield, J. & Shepherd, I. W. Conformation of poly(ethylene oxide) in the solid state, melt and solution measured by Raman scattering. *Polymer* **16**, 505–509 (1975).
- 3 Kjellander, R. & Florin, E. Water structure and changes in thermal stability of the system poly(ethylene oxide)-water. *J. Chem. Soc. Faraday Trans. 1* **77**, 2053–2077 (1981).
- 4 Gemmei-Ide, M., Miyashita, T., Kagaya, S. & Kitano, H. Mid-infrared spectroscopic investigation of the perfect vitrification of poly(ethylene glycol) aqueous solutions. *Langmuir* **31**, 10881–10887 (2015).
- 5 Gemmei-Ide, M., Motonaga, T., Kasai, R. & Kitano, H. Two-step recrystallization of water in concentrated aqueous solution of poly(ethylene glycol). *J. Phys. Chem. B* **117**, 2188–2194 (2013).
- 6 Devanand, K. & Selsler, J. C. Polyethylene oxide does not necessarily aggregate in water. *Nature* **343**, 739–741 (1990).
- 7 Venohr, H., Fraaije, V., Strunk, H. & Borchard, W. Static and dynamic light scattering from aqueous poly(ethylene oxide) solutions. *Eur. Polym. J.* **34**, 723–732 (1998).
- 8 Maconnachie, A., Vasudevan, P. & Allen, G. Molecular dynamics of poly(ethylene oxide) in concentrated solution. *Polymer* **19**, 33–38 (1978).
- 9 Breen, J., Huis, D., de Bleijser, J. & Leyte, J. C. Solvent dynamics in aqueous studied by nuclear magnetic relaxation. *J. Am. Chem. Soc., Faraday Trans.* **84**, 293–307 (1988).
- 10 Hey, M. J. & Ilet, S. M. Water in poly(ethylene oxide): differential scanning calorimetry and nuclear magnetic resonance experiments. *J. Am. Chem. Soc. Faraday Trans.* **86**, 2673–2674 (1990).
- 11 Pochylski, M. & Gapinski, J. Brillouin scattering study of polyethylene glycol/water system below crystallization temperature. *J. Phys. Chem. B* **114**, 2644–2649 (2010).
- 12 Nagoe, A., Kusukawa, H. & Oguni, M. Enhancement of proton ordering in the hexagonal ice in contact with polyethylene glycol crystal. *J. Phys. Chem. C* **119**, 23910–23916 (2015).
- 13 Shimomura, M., Shinyashiki, N. & Yagihara, S. Calorimetric study on structure and property of water in aqueous solutions of poly(ethylene glycol). *Rept. Progr. Polym. Phys. Jpn* **42**, 249–252 (1999).
- 14 Huang, L. & Nishinari, K. Interaction between poly(ethylene glycol) and water as studied by differential scanning calorimetry. *J. Polym. Sci. B Polym. Phys.* **39**, 496–506 (2001).
- 15 Hanger, S. L. & Macrury, T. B. Investigation of phase behavior and water binding in poly(alkylene oxide) solutions. *J. Appl. Polym. Sci.* **25**, 1559–1571 (1980).
- 16 de Vringer, T., Joosten, J. G. H. & Junging, H. E. A study of the hydration of polyoxyethylene at low temperatures by differential scanning calorimetry. *Colloid Polym. Sci.* **264**, 623–630 (1986).
- 17 Bogdanov, B. & Mihailov, M. Melting of water/poly(ethylene oxide) systems. *J. Polym. Sci. Polym. Phys. Ed.* **23**, 2149–2158 (1985).
- 18 Graham, N. B., Zulficar, M., Nwachuku, N. E. & Rashid, A. Interaction of poly(ethylene oxide) with solvents: 2. Water-poly(ethylene glycol). *Polymer* **30**, 528–533 (1989).
- 19 Hey, M. J. & Ilet, S. M. Poly(ethylene oxide) hydration studied by differential scanning calorimetry. *J. Am. Chem. Soc. Faraday Trans.* **87**, 3671–3675 (1991).
- 20 Zobrist, B., Weers, U. & Koop, T. Ice nucleation in aqueous solutions of poly(ethylene glycol) with different molar mass. *J. Chem. Phys.* **118**, 10254 (2003).
- 21 Shinyashiki, N., Shimomura, M., Ushiyama, T., Miyagawa, T. & Yagihara, S. Dynamics of water in partially crystallized polymer/water mixtures studied by dielectric spectroscopy. *J. Phys. Chem. B* **111**, 10079–10087 (2007).
- 22 Sudo, S., Shimomura, M., Kanari, K., Shinyashiki, N. & Yagihara, S. Broadband dielectric study of the glass transition in poly(ethyleneglycol)-mixture. *J. Chem. Phys.* **124**, 044901 (2006).
- 23 Cole, K. S. & Cole, R. H. Dispersion and absorption in dielectrics. I. Alternating current characteristics. *J. Chem. Phys.* **9**, 341–351 (1941).
- 24 Buchner, R., Barthel, J. & Stauber, J. The dielectric relaxation of water between 0°C and 35°C. *Chem. Phys. Lett.* **306**, 57–63 (1999).
- 25 Franks, F. in *Water: a Comprehensive Treatise* (ed. Franks F.) Vol. 7, 215–338 (Plenum, New York, 1982).
- 26 Inada, T. & Lu, S. S. Inhibition of recrystallization of ice grains by adsorption of poly(vinyl alcohol) onto ice surfaces. *Cryst. Growth Des.* **3**, 747–752 (2003).
- 27 Kirkwood, J. G. The dielectric polarization of polar liquids. *J. Chem. Phys.* **7**, 911–919 (1939).
- 28 Shinyashiki, N., Imoto, D. & Yagihara, S. Broadband dielectric study of dynamics of polymer and solvent in poly(vinyl pyrrolidone)/normal alcohol mixtures. *J. Phys. Chem. B* **111**, 2181–2187 (2007).
- 29 Shinyashiki, N., Matsumura, Y., Mashimo, S. & Yagihara, S. Dielectric study on coupling constant of lower critical solution of poly(vinylmethylether) in water. *J. Chem. Phys.* **104**, 6877–6880 (1996).
- 30 Sasaki, K., Matsui, Y., Miyara, M., Kita, R., Shinyashiki, N. & Yagihara, S. Glass transition and dynamics of polymer and water in poly(vinyl pyrrolidone)-water mixture studied by dielectric relaxation spectroscopy. *J. Phys. Chem. B* **120**, 6882–6889 (2016).